23rd International Conference on Material Forming (ESAFORM 2020)

Analysis of Heterogeneous Tests for Sheet Metal Mechanical Behavior

Miguel Guimarães Oliveira[a,b,]*, Sandrine Thuillier[b], António Andrade-Campos[a]

[a]*Centre for Mechanical Technology and Automation (TEMA), Department of Mechanical Engineering, University of Aveiro, 3810-193 Aveiro, Portugal*
[b]*Univ. Bretagne Sud, UMR CNRS 6027, IRDL, F-56100 Lorient, France*

* Corresponding author. Tel.: +351-234-370-830; fax: +351-234-370-953. *E-mail address:* oliveiramiguel@ua.pt

Abstract

Strategies combining heterogeneous mechanical tests and full-field strain measurement techniques are providing increasingly more valuable data, ensuring calibrated constitutive models for the accurate representation of the elastoplastic behavior of sheet metals. However, the accuracy of these strategies is still dependent on many factors, such as the shape of the specimen, the choice of an appropriate strain field measurement technique, or the selection of an identification strategy. Recently, many heterogeneous tests with different specimen shapes and boundary conditions have been proposed using optimization techniques or empirical knowledge. Examples of these specimens include shapes based on cubic splines, notches, holes, slits or even Greek letters. However, the qualitative and quantitative comparison of each heterogeneous test is a difficult task, as studies tend to use different materials and representations of the strain and stress tensors. As a result, the selection of a single heterogeneous test is still a dilemma and a subject under research. Thereby a set of indicators to evaluate and qualitatively rank each heterogeneous test is proposed, calculated through the strain and stress fields on the sheet plane of the specimen, within a virtual (numerical) approach, and investigate its application to steel and aluminum, to account for the material dependency.

Keywords: Sheet metal; Mechanical behavior; Elastoplasticity; Anisotropy; Heterogeneous tests.

1. Introduction

To decrease associated delays and costs, the mechanical design of sheet metal forming parts tends to be nowadays more and more virtual, using numerical simulation. Therefore, the characterization of materials has received increased attention due to the need for precise input data to computational analysis software. The material mechanical behavior can be numerically described through constitutive models and material parameters, which are classically identified using standard homogeneous mechanical tests [1]. In this approach, the strain field is considered homogeneous for tensile conditions along the gauge part of the sample before necking occurs, and in shear conditions, the heterogeneity is neglected. Moreover, from a single classical test, it is difficult to extract a considerable number of parameters, requiring that several tests are performed to

identify many parameters of a single constitutive model [2].

More recently, research has focused on alternative identification methods based on heterogeneous strain fields, measured using full-field experimental techniques that provide significantly more valuable data. However, the accuracy of these alternative methods depends on several factors, such as (i) the shape of the specimen to be used in the mechanical test, (ii) the choice of an appropriate technique of strain field measurement, and (iii) the definition of an identification strategy [3]. These techniques allow the extraction of more information from the strain field developed in the sample, where ideally the use of a single test might be enough to characterize the material behavior. Nonetheless, the selection of a test that demonstrates a rich strain field, both in kind and amount of information is still a topic under research. Additionally, the use of full-field measurement techniques requires inverse methodologies to determine the material

parameters of a specific constitutive model. The identification procedure can consist of minimizing the gap between the experimental and numerical data using an objective function, which depends on the methodology used. As the identification procedure is focused on sheet metals, the thickness of the material is very reduced, and stress levels in the normal direction to the sheet plane are most of the time negligible until localization occurs. Moreover, measuring deformation in the normal direction to the sheet plane is a difficulty in conventional digital image correlation (DIC) techniques. For that reason, studies tend to assume that the material presents an isotropic mechanical behavior in the normal direction to the sheet plane.

Although many challenges exist in this field, the selection of the most suitable heterogeneous tests for sheet metal parameter identification is addressed. In the last decade, the number of new heterogeneous tests has largely increased, with some studies using techniques to optimize the specimen geometry [4,5], while others are based on empirical knowledge [6,7], resulting in geometries with holes, notches or slits. Even though the quantity and quality of heterogeneous tests have increased, a direct comparison is rather difficult as studies use different materials and output data. Souto et al. [8] promoted the use of a standard indicator to evaluate and classify mechanical tests for sheet metal identification, mainly based on the levels of equivalent plastic strain and strain heterogeneity observed in the test. However, this indicator was mainly developed with a specific material and did not account for the specimen sensitivity to anisotropy [9].

To that end, the aim is to qualitatively analyze several heterogeneous tests using different materials and standard indicators, as well as proposing a new indicator to evaluate the test sensitivity to anisotropy, named rotation angle.

2. Analysis of Strain and Stress States

Considering an elastoplastic constitutive model for an anisotropic material, this is composed of an anisotropic yield criterion and hardening rule, either mixed—generally used for reverse loadings—or isotropic, which is considered in this study, limiting the analysis only to monotonic loadings. From classical identification procedures, it is expected that the

Table 1. An overview of strain and stress states observed in mechanical tests for material characterization of sheet metal forming processes, for an isotropic material.

	Strain	Stress
Equibiaxial tension	$\epsilon_2/\epsilon_1 = 1$ $\epsilon_2 > 0, \epsilon_1 > 0$	$\sigma_2/\sigma_1 = 1$ $\sigma_2 > 0, \sigma_1 > 0$
Plane strain tension	$\epsilon_2 = 0$ $\epsilon_1 > 0$	$\sigma_2/\sigma_1 = \nu$ $\sigma_2 > 0, \sigma_1 > 0$
Uniaxial tension	$\epsilon_2/\epsilon_1 = -0.5$ $\epsilon_2 < 0, \epsilon_1 > 0$	$\sigma_2 = 0$ $\sigma_1 > 0$
Shear	$\epsilon_2/\epsilon_1 = -1$ $\epsilon_2 < 0, \epsilon_1 > 0$	$\sigma_2/\sigma_1 = -1$ $\sigma_2 < 0, \sigma_1 > 0$
Uniaxial compression	$\epsilon_2/\epsilon_1 = -2$ $\epsilon_2 < 0, \epsilon_1 < 0$	$\sigma_2 < 0$ $\sigma_1 = 0$

calibration of a constitutive model is based on information from several mechanical tests under distinct strain/stress paths, and to various angles with respect to the material orientation, defined by three orthotropic axes which correspond to the sheet rolling direction (RD), transverse direction (TD) and normal direction (ND).

The selection of the most suitable heterogeneous test is not a straightforward choice and to evaluate the richness of the tests adequate indicators must be used. The equivalent plastic strain $\bar{\epsilon}^p$ is a standard indicator particularly important to measure the level of plastic strain reached during the tests. This indicator can also be used as a measure of the heterogeneity of tests, as a large region of the specimen with high levels of strain is desired, as opposed to strain localization in a reduced region. Additionally, studies have generally used two indicators to analyze the richness of heterogeneous tests, which are based on the eigenvalues of the strain and stress tensors, calculated on the sheet plane: (i) major and minor strain diagram and (ii) major and minor stress diagram, respectively illustrated in Figs. 1a and 1b. Based on these two indicators, the strain and stress states in the sheet plane of the specimens are easily identified. In sheet metal forming processes, the most common observed strain and stress states are the equibiaxial tension, plane strain tension, uniaxial tension, shear, and less commonly uniaxial

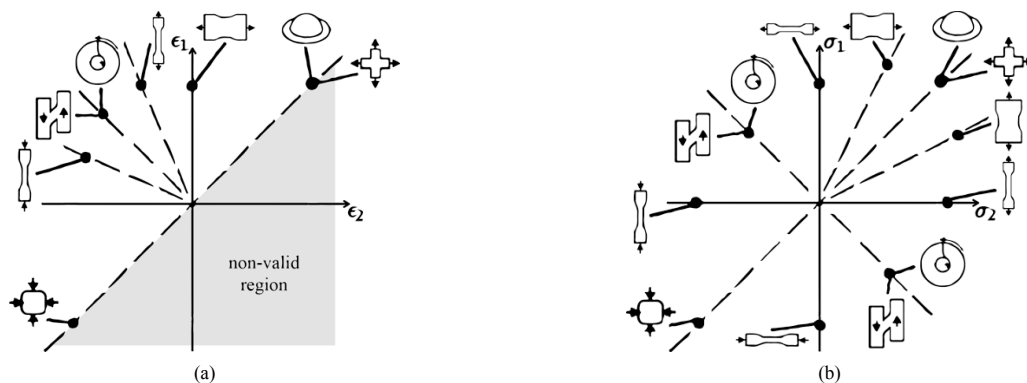(a)   (b)

Fig. 1. An overview of mechanical tests for material characterization of sheet metal forming processes on: (a) major and minor strain, and (b) major and minor stress diagrams (adapted from [10]).

compression. These strain and stress states can be defined by the ratio between the minor ϵ_2 and major ϵ_1 strain, or minor σ_2 and major σ_1 stress in the sheet plane as presented in Table 1—for an isotropic material. However, for anisotropic materials the same strain and stress state can be quantified by different values, therefore the large importance of evaluating the richness of heterogeneous tests for different materials [9].

Furthermore, an indicator able to analyze and quantify the specimen sensitivity to the material anisotropy has not yet been used to evaluate heterogeneous tests. A possible representation for this behavior is the principal angle between the principal stress base and the material orthotropic axes. Its formulation is derived from the Mohr's circle equations for a plane stress condition and is given by

$$\tan 2\beta = \frac{2\sigma_{xy}}{\sigma_{xx} - \sigma_{yy}} \tag{1}$$

where β is a principal angle measured in Mohr's circle and $\sigma_{xx}, \sigma_{yy}, \sigma_{xy}$ are, respectively, the normal stress components in the orthotropic axis x and y, and the shear stress on the sheet plane xy. The solution of Eq. (1) has two roots, β_1 and β_2, respectively corresponding to the principal angle with respect to the major and minor principal stress axis. Nonetheless, by substituting the values of σ_{xx}, σ_{yy}, σ_{xy} in Eq. (1) and solving it for β, its value will correspond to the angle from the material orthotropic axis x to the closest principal stress axis, in such way that it is not possible to know simply from the value of β if the principal angle is associated with the major or minor principal stress axis [11]. Additionally, the values of 2β range between -90º and 90º in Mohr's circle so that β ranges between -45º and 45º in the material frame. Martins et al. [9] applied this formulation presenting the principal angle with respect to the major principal stress axis, to show that a cruciform specimen exhibited a rather wide distribution of the principal angle (from -45º to 135º). However, this formulation ignores the situation when the material point is in a predominant compressive state in Mohr's circle, by only considering the principal angle associated with the major principal stress axis and presents different values for β depending on the shear direction. Moreover, the presented range of values (from -45º to 135º) is not easily associated with the loading angle from the rolling direction, typically analyzed between 0º and 90º for sheet metals.

Therefore, an indicator based on the principal angle formulation that evaluates the sensitivity of the specimen to anisotropy is proposed, by considering the maximum principal stress in absolute value and the range of material orientations typically used to calibrate the material anisotropic behavior. This indicator is named rotation angle γ, and refers to the principal direction associated with the maximum principal stress in absolute value, varies between 0º and 90º, and is given by

$$\gamma = \begin{cases} 45 & \text{if } \sigma_{xx} = \sigma_{yy} \text{ and } \sigma_{xy} \neq 0 \\ 45(1 - q) + q|\beta| & \text{otherwise} \end{cases} \tag{2}$$

where β is the angle in degrees calculated from Eq. (1), and q is an integer with values -1 or 1, calculated as

$$q = \frac{\sigma_{xx} - \sigma_{yy}}{|\sigma_{xx} - \sigma_{yy}|} \frac{|\sigma_1| - |\sigma_2|}{||\sigma_1| - |\sigma_2||} \tag{3}$$

where $|\cdot|$ represents the absolute value. The formulation here presented is arranged in such a way that it can represent all possible states in Mohr's circle, and even though each state has different meanings, it is possible to mathematical reduce them to three different situations, where the rotation angle is: (i) equal to 45º when the value of σ_{xx} is equal to the value of σ_{yy}, and the value of σ_{xy} is different from zero, (ii) equal to $|\beta|$ when the value of σ_{xx} is higher than the value of σ_{yy} for a predominant tensile state ($|\sigma_2| < |\sigma_1|$), and the opposite for a predominant compressive state ($|\sigma_2| > |\sigma_1|$), and lastly, (iii) equal to 90 - $|\beta|$ when the value of σ_{xx} is lower than the value of σ_{yy} for a predominant tensile state ($|\sigma_2| < |\sigma_1|$), and the opposite for a predominant compressive state ($|\sigma_2| > |\sigma_1|$).

3. Heterogeneous Tests and Numerical Models

In this study, three heterogeneous tests reported in the literature are chosen for analysis. In general, these tests were proposed to maximize the strain field heterogeneity observed in the specimen. The selected tests are modeled using symmetry conditions whenever possible and the loading is displacement driven, in order to reduce the computational cost of the numerical simulations. For simplicity, the tests are named Test A, Test B, and Test C, respectively by the order of presentation.

Belhabib et al. [12] proposed a test designed as a hybrid shape between a classical tensile test and a plane tensile test (Fig. 2a). The designed test has been explored by other authors, and because of its simple geometry, it is considered a good basis for this study, avoiding the complexity of the others. Test A is numerically modeled using symmetry conditions in the rolling and transverse directions (one-fourth of the specimen), and the loading direction is aligned with the rolling direction.

Kim et al. [13] proposed a test based on empirical knowledge and trial and error, resulting in a geometry resembling a Greek capital letter sigma Σ (Fig. 2b). The authors showed that this test exhibited various stress states and that combining two tests with different material orientations increased the mechanical information. Test B is numerically modeled using one symmetry condition in the rolling direction (one-half of the specimen), and the loading direction is aligned with the rolling direction.

Jones et al. [14] designed a test via an iterative process where the design was manually adjusted until the geometry met some criteria, such as maximizing stress heterogeneity or the range of strain rates. The optimized geometry resembles a capital letter "D" as presented in Fig. 2c. Test C presents similar boundary conditions to Test B.

The numerical models are two-dimensional, assuming a plane stress formulation. Abaqus/Standard software is used in the finite element analysis [15]. The four-node bilinear plane stress element CPS4R, with reduced integration and stiffness
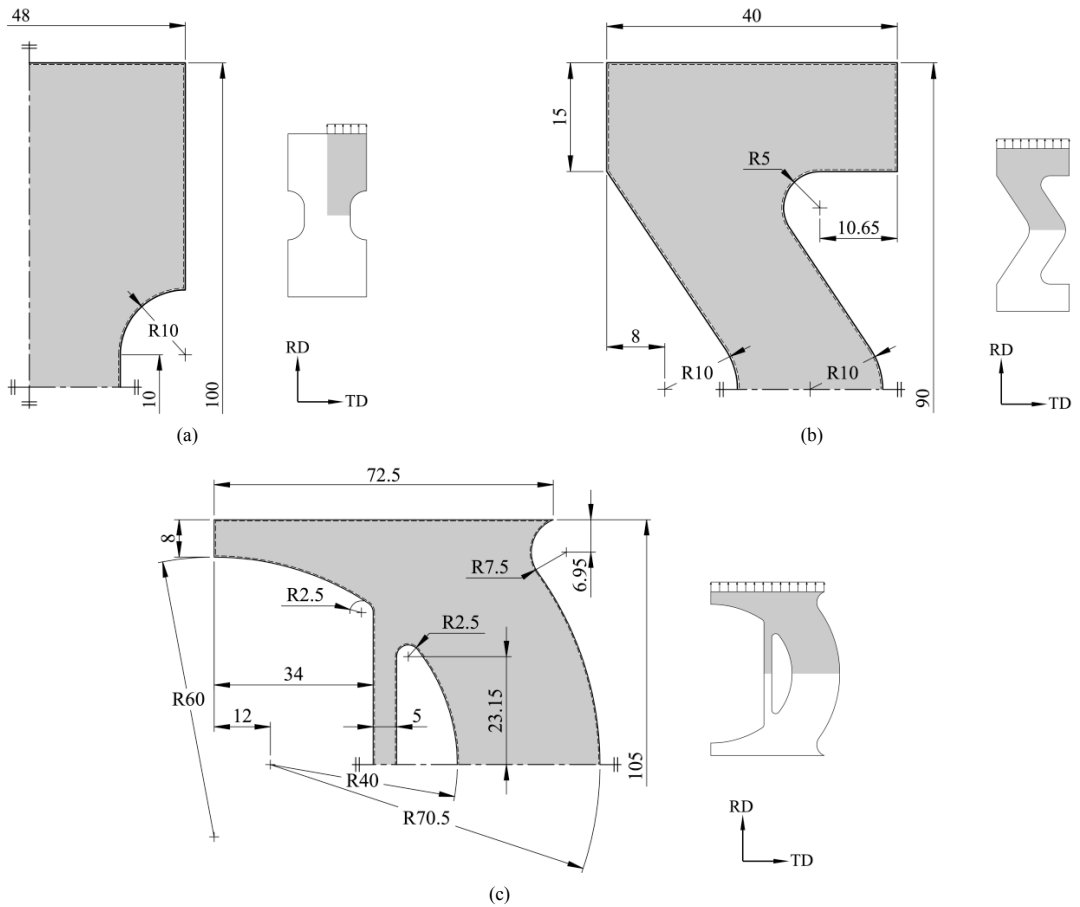
Fig 2. Geometry (dimensions in mm) and boundary conditions of heterogeneous tests considered in this study: (a) Test A, (b) Test B, and (c) Test C.

hourglass control, is used, as well as a large strain formulation. The global mesh seed is of 0.1 elements/mm, with the purpose of obtaining a very fine mesh, providing many material points that resemble a continuous state of the material. To account for the limitations of a subset based DIC, which does not provide information near the free edges of the specimen, the results of the numerical simulations are reported for a region of interest, defined by an arbitrary boundary of 0.25 mm on the free edges of the specimen.

Finally, the numerical simulations are performed with automatic time stepping and maximum increment size of 0.01, and the material behavior is modeled using a user-defined material subroutine, the Unified Material Model Driver for plasticity (UMMDp) [16].

4. Materials and Constitutive Model

4.1. Materials

Two sheet metals are considered in this study, in order to account for the sensitivity of the heterogeneous tests to different materials. A highly textured AA2090-T3 aluminum alloy sheet with a thickness of 1.6 mm [17,18] and a DP600 dual-phase steel with a thickness of 0.8 mm [19]. The mechanical properties of the materials, Young's modulus E, Poisson's ratio ν, normalized yield stress values σ_θ, and

plastic anisotropy coefficients r_θ for different angles θ between the loading and rolling directions are presented in Table 2.

4.2. Constitutive Model

The elastoplastic behavior of the materials is described using the same phenomenological models and formulated assuming additive composition of the strain rate tensor and associated flow rule. The elastic behavior is considered

Table 2. Elastic properties, normalized yield stress values σ_θ and plastic anisotropy coefficients r_θ of AA2090-T3 [17,18] and DP600 [19].

		AA2090-T3	DP600
Elastic	E [GPa]	69	210
	ν	0.33	0.3
σ_θ	σ_0	1.000	1.000
	σ_{45}	0.811	1.020
	σ_{90}	0.910	1.045
r_θ	r_0	0.21	0.89
	r_{45}	1.58	0.85
	r_{90}	0.69	1.12

isotropic, described by Hooke's law and the plastic behavior is considered anisotropic.

The yield condition in plasticity, assuming isotropic hardening can be expressed as

$$f(\boldsymbol{\sigma}, \bar{\epsilon}^{\mathrm{p}}) = \bar{\sigma}(\boldsymbol{\sigma}) - \sigma_{\mathrm{y}}(\bar{\epsilon}^{\mathrm{p}}) = 0 \,, \tag{4}$$

where $\bar{\sigma}(\boldsymbol{\sigma})$ is the equivalent stress defined as a function of the Cauchy stress tensor $\boldsymbol{\sigma}$ and $\sigma_{\mathrm{y}}(\bar{\epsilon}^{\mathrm{p}})$ is the yield stress as a function of the equivalent plastic strain $\bar{\epsilon}^{\mathrm{p}}$. The isotropic hardening is described by the classical Swift's law and can be written as

$$\sigma_{\mathrm{y}}(\bar{\epsilon}^{\mathrm{p}}) = K(\epsilon_0 + \bar{\epsilon}^{\mathrm{p}})^n \,, \tag{5a}$$

$$\epsilon_0 = \left(\frac{\sigma_0}{K}\right)^{1/n} \,, \tag{5b}$$

where K, σ_0 and n are material parameters given in Table 3. The yield surface is described by Yld2000-2d anisotropic yield criterion [20], formulated specifically for plane stress conditions and expressed as

$$2\bar{\sigma}^a = |s_1' - s_2'|^a + |2s_2'' + s_1''|^a + |2s_1'' + s_2''|^a \,, \tag{6}$$

where a is a material parameter that usually assumes the values of 6 or 8, depending on the crystallographic structure of the material, respectively, body-centered cubic (bcc) or face-centered cubic (fcc). s_i' and s_i'' ($i = 1, 2$), are the eigenvalues of the tensors $\boldsymbol{X}'$ and $\boldsymbol{X}''$ obtained after two linear transformations on the deviatoric stress tensor. These transformations can be determined directly from the Cauchy stress tensor as

$$\boldsymbol{X}' = \boldsymbol{L}'\boldsymbol{\sigma} \,, \tag{7a}$$

$$\boldsymbol{X}'' = \boldsymbol{L}''\boldsymbol{\sigma} \,, \tag{7b}$$

where $\boldsymbol{L}'$ and $\boldsymbol{L}''$ are defined as

$$\boldsymbol{L}' = \begin{bmatrix} L_{11}' \\ L_{12}' \\ L_{21}' \\ L_{22}' \\ L_{66}' \end{bmatrix} = \begin{bmatrix} 2/3 & 0 & 0 \\ -1/3 & 0 & 0 \\ 0 & -1/3 & 0 \\ 0 & 2/3 & 0 \\ 0 & 0 & 1 \end{bmatrix} \begin{bmatrix} \alpha_1 \\ \alpha_2 \\ \alpha_7 \end{bmatrix} \,, \tag{8a}$$

$$\boldsymbol{L}'' = \begin{bmatrix} L_{11}'' \\ L_{12}'' \\ L_{21}'' \\ L_{22}'' \\ L_{66}'' \end{bmatrix} = \frac{1}{9} \begin{bmatrix} -2 & 2 & 8 & -2 & 0 \\ 1 & -4 & -4 & 4 & 0 \\ 4 & -4 & -4 & 1 & 0 \\ -2 & 8 & 2 & -2 & 0 \\ 0 & 0 & 0 & 0 & 0 \end{bmatrix} \begin{bmatrix} \alpha_3 \\ \alpha_4 \\ \alpha_5 \\ \alpha_6 \\ \alpha_8 \end{bmatrix} \,, \tag{8b}$$

where α_k ($k = 1,\dots,8$) represent the material-dependent parameters presented in Table 3 for both materials.

5. Results

With the purpose of a fair comparison of the results between the different heterogeneous tests, a stopping

Table 3. Constitutive model parameters for Yld2000-2d anisotropic yield criterion and Swift's isotropic hardening law of AA2090-T3 [17,18] and DP600 [19].

		AA2090-T3	DP600
Yld2000-2d	α_1	0.8603	1.011
	α_2	0.9292	0.964
	α_3	0.9573	1.191
	α_4	0.9768	0.995
	α_5	1.0634	1.010
	α_6	1.0389	1.018
	α_7	-1.2505	0.977
	α_8	1.4496	0.935
	a	8	8
Swift	K [MPa]	646.00	979.46
	σ_0 [MPa]	279.62	355.05
	n	0.227	0.194

condition for the numerical simulations is imposed via a forming limit curve (FLC), which typically quantifies the degree of deformation a sheet metal can undergo without failing. The forming limit curve is represented as a curve in the major and minor strain diagram, also known as forming limit diagram. The forming limit curves are virtually generated based on typical shapes of forming limit curves and the strain hardening exponent n for the maximum value in the plane strain tension region [21]. The resulting maximum displacements for each test and material are 2.025 mm and 2.150 mm for Test A, 1.910 mm and 2.155 mm for Test B, and 2.280 mm and 2.725 mm for Test C, respectively for AA2090-T3 and DP600.

To simplify the analysis, the presented results are from the last increment of the numerical simulations as it can represent a good indication of the strain and stress states observed in the specimen throughout a monotonic loading test [8], and it is proposed that these are represented by three indicators: (i) major and minor strain diagram, (ii) major and minor stress diagram, and (iii) histogram of rotation angle distribution, all in function of the equivalent plastic strain (Figs. 3 and 4). Although the major and minor diagrams might present similar states, they are graphically complementary as some states are more easily observed in one or the other (e.g. uniaxial compression). A novel contribution is the association of the equivalent plastic strain to the major and minor diagrams, which enables a straightforward identification of similar material points between the different indicators. See for example Fig. 3a, where the region with the highest equivalent plastic strain values in the major and minor strain diagram is between uniaxial tension and plane strain tension, in the major and minor stress diagram is closer to uniaxial tension and in the histogram of rotation angle distribution it is located between 0º and 15º. Additionally, it is possible to identify this region within the specimen by observing the contour of equivalent plastic strain represented inside the histogram of rotation angle distribution.
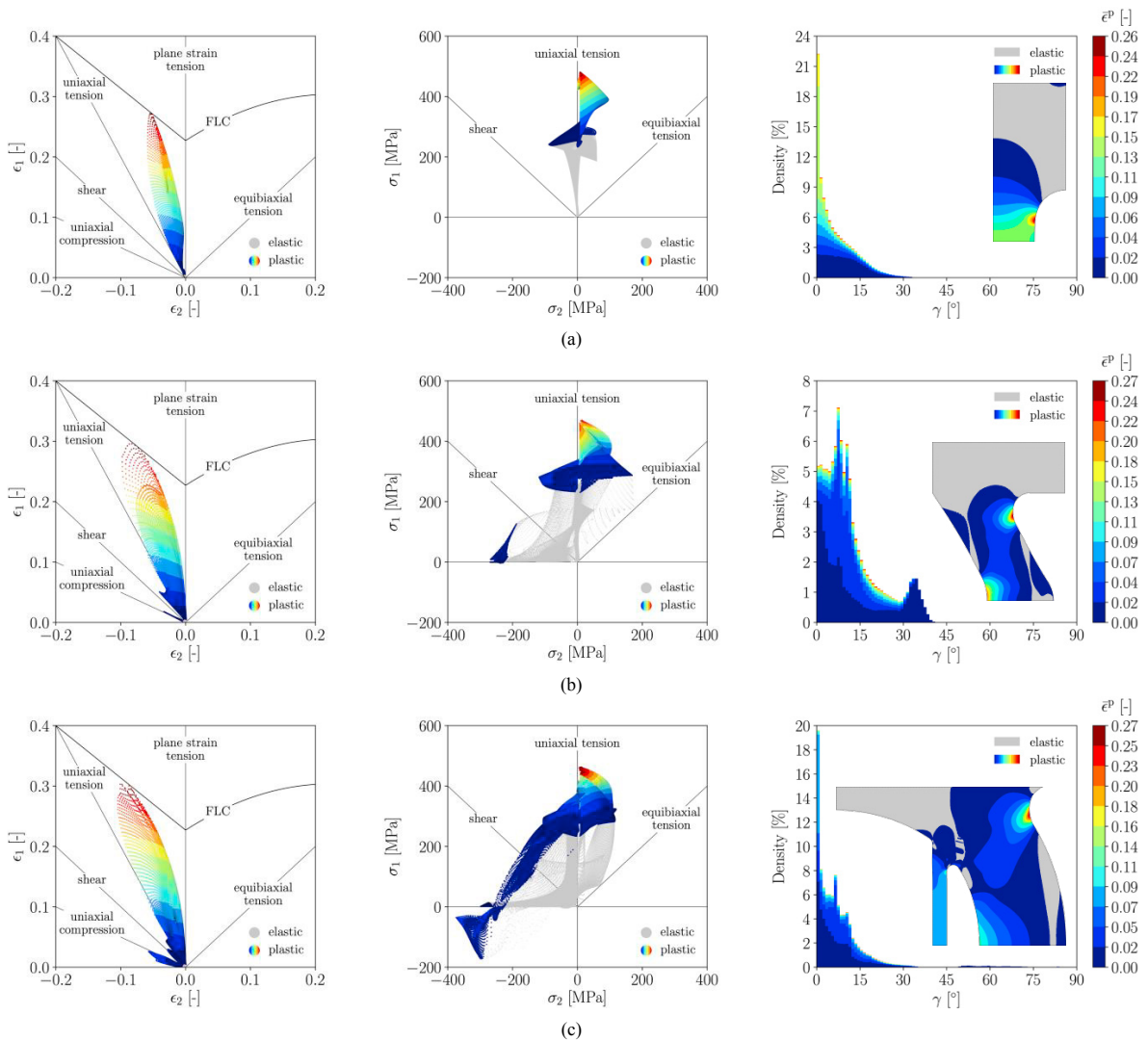
Fig 3. Results of AA2090-T3 represented by major and minor strain diagram (left), major and minor stress diagram (center), and histogram of rotation angle distribution (right): (a) Test A, (b) Test B, and (c) Test C.

Concerning differences observed for the same test with both materials, results confirm the need to evaluate the richness of heterogeneous tests for different materials. See the example of Test A (Figs. 3a and 4a) where it is observed that the specimen is more solicited close to the free edges—tending to a plane strain tension region—for AA2090-T3, as opposed to DP600, where the highest solicitation is observed in the center of the specimen—tending to a uniaxial tension region.

By qualitatively comparing the distribution of strain and stress states, it is observed that Test C covers a wide range of states for both materials, ranging from plane strain tension to uniaxial compression, even though the levels of equivalent plastic strain are low from shear to uniaxial compression (Figs. 3c and 4c). Test B presents a similar range of states as Test C for high levels of equivalent plastic strain. However, for lower levels of equivalent plastic strain, the diversity of states is narrower (Figs. 3b and 4b). Here, it is interesting to observe that the transition from shear to uniaxial compression

is not continuous, limiting a quantitative evaluation based on the maximum and minimum values of the major and minor strain or stress ratio of the whole specimen. In opposition, Test A presents a lower range of states, mainly in the uniaxial tension to plane strain tension regions, particularly limited by their geometric nature. Therefore, it is possible to consider that, according to the major and minor strain or stress diagrams, Test C is qualitatively better than Test A and Test B, as it presents a wider range of strain and stress states—both for low and high levels of equivalent plastic strain.

Analyzing the results of the rotation angle distribution for all tests it is observed that the range of values is mainly located on the left side of the histogram (from 0º to 45º), which reflects the alignment of the loading and rolling directions in the three tests. Nonetheless, Test B and Test C present some material points on the right side of the histogram, even if for small values of equivalent plastic strain and low density of material points. Out of the three tests,
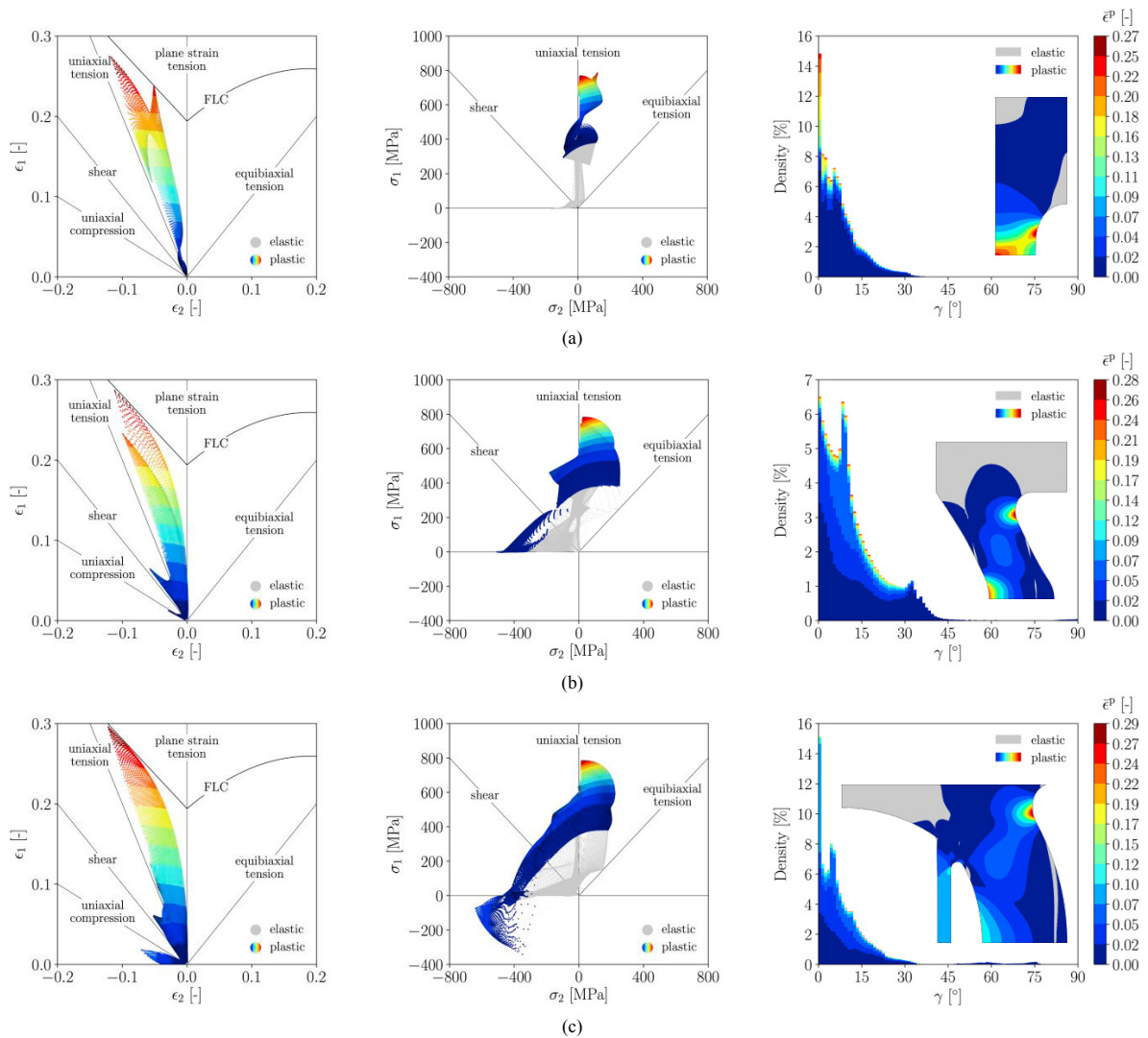
Fig 4. Results of DP600 represented by major and minor strain diagram (left), major and minor stress diagram (center), and histogram of rotation angle distribution (right): (a) Test A, (b) Test B, and (c) Test C.

Test B presents a more spread density of material points with high values of equivalent plastic strain between 0º and 45º. Hence, Test B can be considered, according to the distribution of the rotation angle, the most sensitive test to anisotropy out of the three tests.

Globally, Test A can be considered the least interesting test, while it is rather difficult to qualitatively rank the interest of Test B and Test C. The first appears to outperform the last in the distribution of the rotation angle, but the opposite is observed for the major and minor strain or stress diagrams.

6. Conclusion

A qualitative analysis of different heterogeneous tests is performed based on distinct indicators of the mechanical information extracted from the tests. An indicator based on the principal direction associated with the maximum principal stress in absolute value and the material frame is proposed to evaluate the sensitivity of tests to anisotropy. The simultaneous use of the major and minor strain diagram, major and minor stress diagram, and histogram of rotation angle distribution, in function of the equivalent plastic strain, to evaluate the richness of heterogeneous tests is an original contribution and provides a good basis to qualitatively rank heterogeneous tests. Future work will deal with the design of a new indicator able to quantitatively rank heterogeneous tests independently of the considered materials.

References

[1] Souto N, Andrade-Campos A, Thuillier S. Material parameter identification within an integrated methodology considering anisotropy, hardening and rupture. J Mater Proc Tech 2015;220:157-172.

[2] Barlat F, Aretz H, Yoon J, Karabin M, Brem J, Dick R. Linear transformation-based anisotropic yield functions. Int J Plast 2005;21(5):1009-1039.

[3] Prates P, Pereira A, Sakharova N, Oliveira M, Fernandes J. Inverse strategies for identifying the parameters of constitutive laws of metal sheets. Adv Mater Sci Eng 2016;1-18.

[4] Rossi M, Badaloni M, Lava P, Debruyne D, Pierron F. A procedure for specimen optimization applied to material testing in plasticity with the virtual fields method. AIP Conf Proc 2016;1769:1-6.

[5] Souto N, Andrade-Campos A, Thuillier S. Mechanical design of a heterogeneous test for material parameters identification. Int J Mater Form 2017;10(3):353-367.

[6] Pottier T, Vacher P, Toussaint F, Louce H, Couder T. Out-of-plane testing procedure for inverse identification purpose: application in sheet metal plasticity. Exp Mech 2012;52(7):951-963.

[7] Liu W, Guines D, Leotoing L, Rganeau E. Identification of sheet metal hardening for large strains with an in-plane biaxial tensile test and a dedicated cross specimen. Int J Mech Sci 2015;101:387-398.

[8] Souto N, Thuillier S, Andrade-Campos A. Design of an indicator to characterize and classify mechanical tests for sheet metals. Int J Mech Sci 2015;101:252-271.

[9] Martins J, Andrade-Campos A, Thuillier S. Calibration of anisotropic plasticity models using a biaxial test and the virtual fields method. Int J Solids and Struct 2019;172-173:21-37.

[10] Brosius A, Yin Q, Güner A, Tekkaya A. A new shear test for sheet metal characterization. Steel Res Int 2011;82(4):323-328.

[11] Hibbeler RC. Mechanics of Materials. 8th ed. New Jersey: Pearson Prentice Hall; 2011.

[12] Belhabib S, Haddadi H, Gaspérini M, Vacher P. Heterogeneous tensile test on elastoplastic metallic sheets: comparison between FEM simulations and full-field strain measurements. Int J Mech Sci 2008;50(1):14-21.

[13] Kim J, Barlat F, Pierron F, Lee M. Determination of anisotropic plastic constitutive parameters using the virtual fields method. Exp Mech 2014;54(7):1189-1204.

[14] Jones E, Carrol J, Karlson K, Kramer S, Lehoucq R, Reu P, Turner D. Parameter covariance and non-uniqueness in material model calibration using the virtual fields method. Comput Mater Sci 2018;152:268-290.

[15] Dassault Systèmes. Abaqus 2017 Documentation. 2017.

[16] Takizawa H, Oide K, Suzuki K, Yamanashi T, Inoue T, Ida T, Nagai T, Kuwabara T. Development of the user subroutine library "Unified Material Model Driver for plasticity (UMMDp)" for various anisotropic yield functions. J Phys Conf Ser 2018;1063.

[17] Abedini A, Butcher C, Rahmaan T, Worswick M. Evaluation and calibration of anisotropic yield criteria in shear loading: constraints to eliminate numerical artefacts. Int J Solids and Struct 2015;151:118-134.

[18] Yoon J, Barlat F, Dick R, Karabin M. Prediction of six or eight ears in a drawn cup based on a new anisotropic yield function. Int J Plast 2006;22(1):174-193.

[19] Ozturk F, Toros S, Kilic S. Effects of anisotropic yield function on prediction of forming limit diagrams of DP600 advanced high strength steel. Procedia Eng 2014;81:760-765.

[20] Barlat F., Brem J, Yoon J, Chung K, Dick R, Lege D, Pourboghrat F, Choi S, Chu E. Plane stress yield function for aluminum alloy sheets – part 1: theory. Int J Plast 2003;19(9):1297-1319.

[21] Paul S. Theoretical analysis of strain and stress-based forming limit diagrams. J Strain Anal Eng 2012;48(3):177-188.